UNIVERSIDADE ESTADUAL DE CAMPINAS
SISTEMA DE BIBLIOTECAS DA UNICAMP
REPOSITÓRIO DA PRODUÇÃO CIENTIFICA E INTELECTUAL DA UNICAMP

Versão do arquivo anexado / Version of attached file:

Versão do Editor / Published Version

Mais informações no site da editora / Further information on publisher's website:

https://www.osapublishing.org/ol/abstract.cfm?uri=ol-31-13-2069

DOI: 10.1364/OL.31.002069

Direitos autorais / Publisher's copyright statement:

Efficient 1 GHz Ti:sapphire laser with improved broadband continuum in the infrared

Giovana T. Nogueira and Flavio C. Cruz

Instituto de Física Gleb Wataghin, Universidade Estadual de Campinas, CP 6165, Campinas, SP, 13083-970, Brazil

We demonstrate a 1 GHz prismless femtosecond Ti:sapphire ring laser that emits 890 mW for 7.6 W of pump power over a continuum extending from 585 to 1200 nm at −20 dB below the maximum. A broadband continuum is obtained with the net cavity group delay dispersion having −50 to 100 fs^2 oscillations from 700 to 900 nm. Further broadening is obtained by use of a slightly convex cavity mirror that increases self-phase modulation. Approximately 17% (75%) of the intracavity (output) power is generated in single pass through the crystal, outside the cavity bandwidth, and concentrated in the low-gain IR from 960 to 1200 nm. © 2006 Optical Society of America

OCIS codes: 140.7090, 320.7160, 120.3940.

Femtosecond lasers are the basis of optical frequency combs, which have revolutionized frequency metrology and precision measurements in the past few years.[1] They have been used, for example, for direct measurements of frequencies of several hundred terahertz,[2] in optical atomic clocks,[3] and for phase-sensitive nonlinear optics experiments.[4] For measurement and control of the carrier-to-envelope offset frequency (f_{ceo}) in optical frequency combs, a femtosecond laser whose spectrum covers one octave is desirable. Although the use of a microstructure fiber offers a solution to this, there are problems for continuous and long-term operation, which is important for clocks and other applications. In this way, the advent of femtosecond lasers (in particular Ti:sapphire) emitting a broadband continuum[5–9] has attracted interest. These lasers have been demonstrated with stationary-wave, longer cavities operating with prisms to compensate for group delay dispersion (GDD) or with short, traveling-wave, prismless ring cavities that use chirped mirrors. In the first case, repetition rates are typically smaller, near 100 MHz or below, while the second case allows for repetition rates of 1 GHz or higher, which are often preferred for optical frequency measurements. The measurement and stabilization of f_{ceo} has also been demonstrated with such lasers.[7–9] In this Letter we report what to our knowledge is the most broadband femtosecond spectrum to date, obtained from a Ti:sapphire laser whose spectrum covers from 585 to 1200 nm at a level of −20 dB below the maximum. It operates stably with an output power of 890 mW for 7.6 W of pump power, and a repetition rate near 1 GHz.

The main laser cavity described here consists of a four-mirror bow-tie ring cavity comprising two curved mirrors [including the input coupler (IC)], with broadband high reflecting (HR) coatings and radius of curvature of 3 cm, a HR flat mirror, and a flat output coupler (OC) with a transmission of 2% from 730 to 870 nm. The cavity configuration is similar to those used in Refs. 5 and 9, but we used different mirrors and a longer crystal. All mirrors are commercially available[10] and chirped, with a GDD of −60 fs^2

from 720 to 990 nm, excluding the OC. In another cavity configuration the HR flat mirror has been replaced by a broadband HR convex mirror ($r=1$ m) to enhance self-phase modulation[5] (SPM). A 3 mm long Brewster-cut Ti:sapphire crystal is placed at the cavity's tighter waist between the curved mirrors. The Ti^{3+} concentration is such that 70% of the power from a single-frequency pump laser at 532 nm is absorbed. The net cavity GDD is shown in Fig. 1. Curve a is an average of four traces obtained by white-light interferometry,[11] including the two curved mirrors, the convex mirror, and the Ti:sapphire crystal, but not the OC. Curve b is the calculated GDD based on the curves of the same mirrors provided by the manufacturer, and combined with a Ti:sapphire crystal flat GDD of 174 fs^2 (Ref. 12). Curve c is the same as b but with the convex mirror replaced by the HR flat mirror. Curve d is the calculated GDD of the OC only, also provided by the manufacturer.[10] A few comments can be made from Fig. 1: (1) the positive GDD of the crystal is nearly compensated by the negative GDD of the chirped mirrors, giving small negative net GDD in certain wavelength regions (small negative net
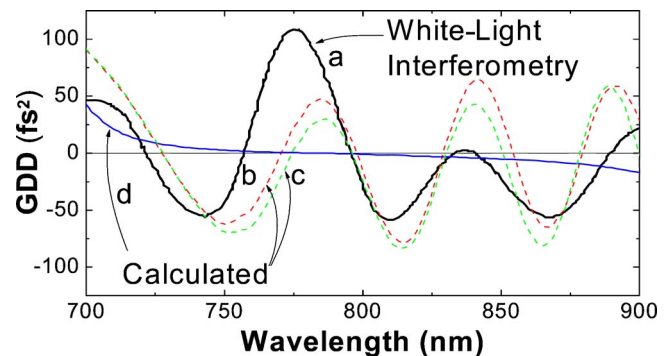

Fig. 1. (Color online) Net GDD of the four-mirror bow-tie laser cavity, including the crystal and excluding the output coupler. Curve a, measurement by white-light interferometry, with convex mirror included; b, calculated GDD of mirrors based on curves provided by manufacturer (convex mirror included), combined with a Ti:sapphire 3 mm crystal flat GDD of 174 fs^2 (Ref. 12); c, same as b, but with convex mirror replaced by HR flat mirror; d, calculated GDD of the OC provided by the manufacturer.

© 2006 Optical Society of America

GDD is known to give short pulses[13,14]); (2) oscillation compensation has not been important for the generation of a broadband spectrum; and (3) the net GDD is even positive near the Ti:sapphire gain peak, from 760 to 800 nm.

In addition to the cavity described above, we have also built two ring cavities with six mirrors and a reduced repetition rate of 920 MHz. These cavities differ from the former one by the addition of two HR flat chirped mirrors (-70 fs^2 from 720 to 1000 nm, oscillation compensated[10]) and by a different chirped IC (-40 fs^2 from 700 to 850 nm, HR from 650 to 900 nm). They differ from each other in using a flat HR chirped mirror (-60 fs^2) or an unchirped mirror, such that the net cavity GDD (mirrors and crystal) amounted to -120 and -60 fs^2, respectively. The convex mirror was not used. In either case we could not generate a broadband continuum. Curve a in Fig. 2 corresponds to the laser spectrum for either of these six-mirror cavities, showing a Gaussian profile centered at 777 nm, with a FWHM of 10 nm. Curve b corresponds to the spectrum for the four-mirror cavity when the flat HR mirror was used instead of the convex one. In curves c and d the convex mirror has been used. Curves c and d differ from each other only by changes in the cavity alignment, as we explain below.

A significant difference between the six-mirror cavities with excess negative net GDD (curve a in Fig. 2) and the four-mirror one (curves b–d) in Fig. 2 is their sensitivity for alignment and operation. We found that mode locking was more difficult to achieve for the six-mirror cavities, requiring careful adjustment of the curved mirror angles. Precise positioning of the curved mirrors with respect to the crystal was also necessary to eliminate a cw component. On the other hand, the four-mirror cavity mode locks easily, with considerably fewer critical adjustments. No instabilities associated with possible *Q*-switching operation were observed, as can be seen from the inset in Fig. 3, which shows a beat signal at the laser repetition rate. For this four-mirror cavity using the convex mirror and for input powers above 6 W, as the

Fig. 3.   (Color online) Laser output powers for the four-mirror bow-tie cavity. Curve a, cw operation; b, mode-locked operation in the first region discussed in the text, corresponding to curve b of Fig. 2; c, mode-locked operation in the second region discussed in the text (curve d in Fig. 2). Inset, Beatnote at laser repetition rate.

curved mirror opposing the IC is moved toward the crystal, three distinct regions can be identified near the inner edge of the 2.6 mm long stability range for the distance between these curved mirrors. In the first region the laser oscillates mode locked in one direction of the ring cavity. An intermediate region is more sensitive to alignment, with mode-locked oscillation alternating between both directions of the ring cavity, without any cw component. The third region is similar to the first, but the laser oscillates in the other direction with respect to the first region. We note that there are similarities between this description and the one given in Ref. 5. Curves b and c in Fig. 2 are typical spectra for the laser operating either in the first or third regions. These spectra are quite similar to those in Refs. 5 and 9 and are obtained either with the flat or convex HR mirror, showing that a broadband spectrum is primarily obtained when the net cavity GDD is small. Curve d in Fig. 2 corresponds to operation in the second region using the convex mirror, which adds further broadening. We have not determined if these three regions are specifically associated with using the convex mirror, and for input powers below 6 W only the first and third regions are observed.

The spectrum of curve d in Fig. 2 is quite remarkable, extending from 585 to 1200 nm at the -20 dB level from the maximum at 986 nm, or at -10 dB with respect to the power at 800 nm. Since in our measurements the laser oscillation direction has always been opposed to the pump direction, the light that leaves the crystal reflects in the IC and is transmitted through the OC. The peaks in the laser spectrum at 660, 680, and 986 nm in curves c and d in Fig. 2 occur at maxima in the OC transmission spectrum, and the dips at 1190 and 1250 nm are simply due to minima of the IC reflection spectrum. Assuming that light outside the cavity bandwidth is generated in only a single pass through the crystal, mainly by SPM and also by the Ti:sapphire gain, a considerable increase in output power would be possible simply if the transmission or reflection of the IC or OC could be optimized. If the spectrum of curve d in Fig. 2 is corrected by the reflectivity of the IC and OC
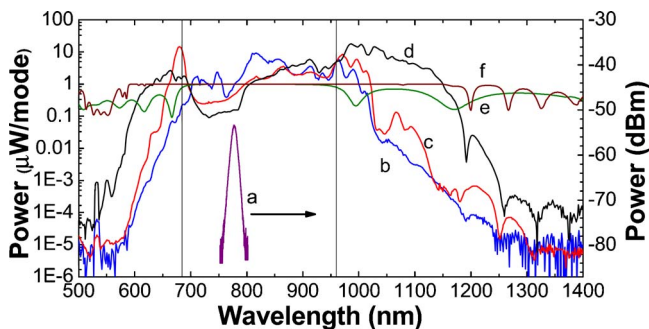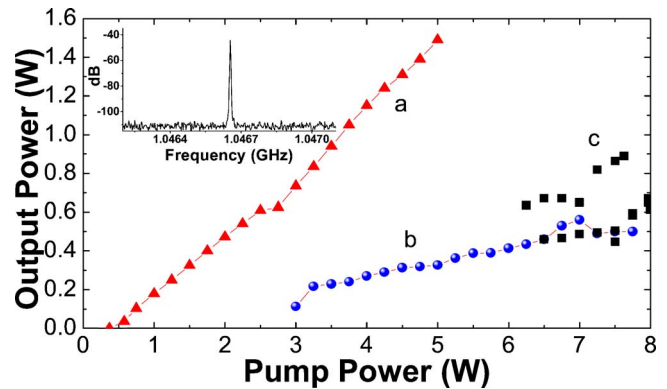

Fig. 2.   (Color online) Output spectra for the Ti:sapphire mode-locked lasers. Curve a, normal mode-locked laser using the six-mirror ring cavities with excess negative GDD (see text); b, broad spectrum obtained with the four-mirror cavity with small net GDD; c and d, spectra when a convex mirror ($r = 1$ m) replaces the HR flat mirror for two different alignment conditions; e and f, reflectivity of the OC and IC (read using the numbers on left y axis). Vertical bars, laser cavity bandwidth (see text).

(Fig. 2), we obtain the intracavity power spectrum. By defining a cavity bandwidth from 685 to 960 nm, corresponding to points where the transmission of the OC increases to 20% (vertical lines in Fig. 2), we integrated the intracavity power spectrum to compute which fractions are generated both inside and outside the cavity bandwidth (e.g., in single pass through the crystal). We thus obtain the impressive number that 17% of the intracavity power is generated in single pass mainly by SPM and also gain in the crystal. This fraction increases to 75% for the available power outside the cavity. Most of this power is concentrated in the IR portion of the spectrum, from 960 to 1200 nm. It is possible that the broadband chirped mirrors, with HR coatings and negative GDD extending up to 990 nm, the tight focus in a relatively long crystal, and high-order dispersion all play important roles for this improved generation in the IR.

We have also replaced the OC by another mirror with transmission reduced to 1% over the same spectral extension. In this case, the output power has been nearly the same, and the spectrum is slightly narrower. Using a microstructure fiber, previously employed to generate a broadband continuum from the six-mirror cavity lasers, does not cause any further spectral broadening.

Figure 3 shows power curves for the four-mirror cavity. Curve a is for cw operation, with the cavity optimally aligned in the center of its stability curve. The high slope efficiency of 32% (1.5 W for 5 W pumping) and the low threshold (350 mW) are consequences of the compact design with tight waist size in the crystal. Curve b corresponds to the spectrum of curve c in Fig. 2, obtained in the first region discussed above. We obtain a slope efficiency of 7% and a threshold near 3 W for mode-locked operation. Approximately 330 mW (560 mW) is obtained for 5 W (7 W) of pump power. Although in this region cw oscillation can occur for pump powers lower than 3 W, it has not been observed above that pump power. Curves a–c in Fig. 2 were obtained for 5 W pumping, and curve d was obtained for 8 W. However, there was no significant variation of the output spectrum as a function of input power. Curve c in Fig. 3 corresponds to the broadest spectrum of curve d in Fig. 2, obtained in the second region discussed above. It shows a bistable regime with hysteresis, with the power sometimes changing discontinuously in a way that depends on whether the pump power is increased or decreased. By changing only the pump power, we can also observe two output powers for the same pump power. Mode-locked operation in this second region has always led to a broad continuum. For the six-mirror cavities we obtained output powers of 550 mW for 5 W of pump power.

In summary, we have demonstrated a 1 GHz fs Ti:sapphire prismless laser that emits a broadband continuum with an improved IR spectrum. Approximately 75% of the output power is generated in a single pass through the crystal, mainly by SPM, and is concentrated in the spectral region from 960 to 1200 nm, outside the laser cavity bandwidth, and where the Ti:sapphire gain is low. The primary condition for broadband spectrum is attributed to operating this compact laser cavity at small negative net GDD. However, precise oscillation compensation has not been important, and the net cavity GDD is found to be positive near the Ti:sapphire gain peak. Using a slightly convex mirror contributed to additional broadening. We expect that this ultrabroadband laser with improved IR spectrum will make it easier to measure and stabilize the laser carrier-to-envelope offset frequency by using nonlinear $f-2f$ spectrometers[1] without using microstructure photonic fibers.

References

1. J. Ye and S. T. Cundiff, eds., *Femtosecond Optical Frequency Comb Technology* (Springer, 2005).
2. Th. Udem, J. Reichert, R. Holzwarth, and T. W. Hänsch, Opt. Lett. **24**, 881 (1999).
3. S. A. Diddams, Th. Udem, J. C. Bergquist, E. A. Curtis, R. E. Drullinger, L. Hollberg, W. M. Itano, W. D. Lee, C. W. Oates, K. R. Vogel, and D. J. Wineland, Science **293**, 825 (2001).
4. U. Morgner, R. Ell, G. Metzler, T. R. Schibli, F. X. Kärtner, J. G. Fujimoto, H. A. Haus, and E. P. Ippen, Phys. Rev. Lett. **86**, 5462 (2001).
5. A. Bartels and H. Kurz, Opt. Lett. **27**, 1839 (2002).
6. R. Ell, U. Morgner, F. X. Kärtner, J. G. Fujimoto, E. P. Ippen, F. Scheuer, G. Angelow, T. Tschudi, M. J. Lederer, A. Boiko, and B. Luther-Davis, Opt. Lett. **26**, 373 (2001).
7. T. M. Fortier, D. J. Jones, and S. T. Cundiff, Opt. Lett. **28**, 2198 (2003).
8. L. Matos, D. Kleppner, O. Kuzucu, T. R. Schibli, J. Kim, E. P. Ippen, and F. X. Kaertner, Opt. Lett. **29**, 1683 (2004).
9. T. M. Fortier, A. Bartels, and S. A. Diddams, Opt. Lett. **31**, 1011 (2006).
10. Mirrors are from Layertec (www.layertec.com) and quoted GDDs are from the manufacturer.
11. J.-C. Diels and W. Rudolph, *Ultrashort Laser Pulse Phenomena: Fundamentals, Techniques, and Applications on a Femtosecond Timescale* (Academic, 1996).
12. S. Barkus, C. G. Durfee III, M. M. Murnane, and H. C. Kapteyn, Rev. Sci. Instrum. **69**, 1207 (1998).
13. T. Brabec, Ch. Spielmann, and F. Krausz, Opt. Lett. **17**, 748 (1992).
14. Y. Chen, F. X. Kärtner, U. Morgner, S. H. Cho, H. A. Haus, E. P. Ippen, and J. G. Fujimoto, J. Opt. Soc. Am. B **16**, 1999 (1999).